

# Graph Convolutional Networks based on Manifold Learning for Semi-Supervised Image Classification

Lucas Pascotti Valem , Daniel Carlos Guimarães Pedronette   
and Longin Jan Latecki .

**Abstract**—Due to a huge volume of information in many domains, the need for classification methods is imperious. In spite of many advances, most of the approaches require a large amount of labeled data, which is often not available, due to costs and difficulties of manual labeling processes. In this scenario, unsupervised and semi-supervised approaches have been gaining increasing attention. The GCNs (Graph Convolutional Neural Networks) represent a promising solution since they encode the neighborhood information and have achieved state-of-the-art results on scenarios with limited labeled data. However, since GCNs require graph-structured data, their use for semi-supervised image classification is still scarce in the literature. In this work, we propose a novel approach, the Manifold-GCN, based on GCNs for semi-supervised image classification. The main hypothesis of this paper is that the use of manifold learning to model the graph structure can further improve the GCN classification. To the best of our knowledge, this is the first framework that allows the combination of GCNs with different types of manifold learning approaches for image classification. All manifold learning algorithms employed are completely unsupervised, which is especially useful for scenarios where the availability of labeled data is a concern. A broad experimental evaluation was conducted considering 5 GCN models, 3 manifold learning approaches, 3 image datasets, and 5 deep features. The results reveal that our approach presents better accuracy than traditional and recent state-of-the-art methods with very efficient run times for both training and testing.

## I. INTRODUCTION

Over the last years, the fast development of data acquisition technologies and the huge growth of multimedia collections (e.g. image, video, music, and others) have made the use of classification systems indispensable [1]. There is a wide range of different applications, including person re-identification [2], diagnosis of diseases [3], facial recognition [4], remote sensing [5], object identification [6], and various others. However, despite the significant recent advances in feature extraction methods, effectively retrieving multimedia data still remains a challenge in various scenarios. Such complexity is mainly associated to the diverse aspects involved in human visual perception, which usually can not be encoded by a single visual feature [7], [8].

Due to the huge success of deep learning, especially based on Convolutional Neural Networks (CNNs), multiple models applied to both image and video content, have been proposed [9]–[12]. Despite the remarkable results mainly supported by CNN models [9]–[11], [13], [14], most methods

demand a high amount of data to be trained [13], [15]. The availability of supervised training data is often a challenge due to the need for labeling a lot of information, which is expensive and time-consuming [16]. With the objective of easing up the process of labeling data and not requiring manual intervention for this task, there are researches that propose to assist the process of labeling with automatic stages [15]. However, in spite of these possibilities, the process of obtaining labeled data remains a challenge for multiple tasks [16], since the amount of multimedia data available increases much faster than the amount of labeled data that can be obtained for it [17].

In this scenario, various learning paradigms have been attracting increasing attention in order to deal with the scarcity of labeled data. Unsupervised [18]–[21] and semi-supervised [22]–[24] strategies often offer attractive solutions. While the unsupervised approaches require no labeled data at all, the semi-supervised ones require a small set of labeled data. A recent trend is given by weakly supervised learning [25], which is a broad taxonomy that covers different strategies often divided into three main categories: (i) incomplete supervision: where only a subset of the training data is labeled, a part of the other subset can be labeled considering active learning or semi-supervised learning; (ii) inexact supervision: the available labels are used to create rules and constraints (heuristics) on the training data; and (iii) inaccurate supervision: there are wrong or low-quality labels and the idea is to identify the potential mislabeled instances and to correct or remove them.

In general, incomplete supervision often depicts scenarios very close to real-world applications, modeled by Semi-Supervised Learning (SSL) which considers reliable but limited labeled data. Over the last years, SSL approaches have also witnessed huge advances, mainly supported by Graph Convolutional Networks (GCNs) [24]. Different from traditional CNN models, which generally operate through convolutions in the Euclidean space, the GCN models allow convolution operations in non-Euclidean domains defined by graph-based structures [24], [26]. Although very effective, CNN models often ignore contextual information such as neighborhood references and the relationship between the elements in the dataset. Furthermore, CNNs are often applied to 2D and 3D data (e.g., images and videos) and are generally not easily applicable to 1D feature vectors, unless some data processing or conversion is done in the original data [27].

The GCNs exploit multidimensional feature vectors and graph-based neighborhood structures to learn more effective representations. Due to these aspects, the GCNs have been recently applied for graph-based data on semi-supervised

L. P. Valem and D. C. G. Pedronette are with the Department of Statistics, Applied Math. and Computing, State University of São Paulo, Rio Claro, Brazil (e-mail: {lucas.valem, daniel.pedronette}@unesp.br).

L. J. Latecki is with Department of Computer and Information Sciences, Temple University, Philadelphia, USA (e-mail: latecki@temple.edu).

learning tasks, achieving state-of-the-art results. Several GCN variations have been proposed with relevant results [28]–[31]. The use of GCN has many different applications. There are some recent works that exploit graph learning for question and answer systems [32], including conversational image search [33].

While it offers an effective contextual representation learning strategy, GCN models require graph-structured data. The graph data is inherently available in some domains, but needs to be inferred or constructed in others [34]. Consequently, several methods have been proposed for graph-structured data as citation datasets [28]–[31], [35]–[37], but only a few approaches have been proposed for image and multimedia data [38]–[41]. In most cases, the most direct approach is to create a  $k$ -nearest neighbor graph. However, the GCN models are sensitive to the input graph, in the sense that a more effective classification depends on the edges between nodes of the same class.

In this paper, we propose a novel GCN-based approach, the Manifold-GCN, for image classification in semi-supervised scenarios, with limited labeled data. Deep features are extracted for image representation employing transfer learning by CNNs and Vision Transformers (ViT) models. Ranking structures are computed and used as input by unsupervised manifold learning algorithms based on these extracted features. In general, manifold Learning approaches aim to capture and exploit the intrinsic manifold structure to compute a more effective distance/similarity measure [42]. In this work, we consider recent unsupervised manifold learning methods to provide more effective similarity measures using rank-based formulations.

The manifold learning methods produce more effective ranking results, i.e., improved neighbor sets, which are exploited for building the input graph of the GCN model. In addition to constructing kNN graphs, the use of reciprocal kNN graphs is proposed. The main hypothesis of the paper is that the use of manifold learning to improve the graph structure provided as the input of the Graph Convolutional Network (GCN) can further improve the classification results obtained. This work proposes and validates this hypothesis on different manifold learning and recent GCN approaches.

We can highlight the main contributions of our work as follows: (i) novel ways to learn the graph structures that improve GCN image classification; (ii) the use of reciprocal kNN graph in order to provide a more reliable graph for GCNs. There are very few works that employ kNN graphs [34] or manifold learning [35] for GCNs. In [34] the traditional kNN graph is employed and [35] uses manifold learning, but in both works no image data is considered. Other few works have recently employed GCN models on image classification [38]–[41]. However, to the best of our knowledge, this is the first work that exploits both manifold learning and reciprocal kNN graphs for GCN-based semi-supervised image classification. In addition, it combines powerful contextual modeling given by GCN models with effective representations given by CNNs and ViT features.

There are many applications of the proposed approach. The improvement of classification results using GCNs may benefit

many different areas, especially when there is limited labeled data. For example: person re-identification [2] and diagnosis of diseases [3]. The Manifold-GCN can be employed in scenarios where the graph data is not previously available by building the graph from the features and employing manifold learning.

A wide experimental evaluation was conducted in order to assess the effectiveness of the proposed approach. The experimental results were obtained on 3 public datasets. We evaluated the impact of different GCN models combined with different manifold learning methods. The experimental results demonstrate the effectiveness of the proposed approach and the gains on combining manifold learning and reciprocal kNN graphs.

This paper is organized as follows. Section II presents the related work, while Section III presents the formal definition of semi-supervised learning. Section IV describes our proposed approach, the ManifoldGCN. Section V presents the GCNs and manifold learning methods considered. Section VI reports the experimental evaluation. Finally, Section VII states conclusions and considers possible future works.

## II. RELATED WORK

This section presents an overview of the methods proposed for semi-supervised image classification over recent years and their main ideas, especially regarding deep learning.

Semi-supervised approaches perform training considering both labeled and unlabeled data, which is advantageous in multiple scenarios where there is little labeled data [43]. Some of them rely on the generation of pseudo-labels [44]. Among the traditional methods for generating pseudo-labels, we can cite: Label Spreading [45] and Pseudo-label [46]. There are also several supervised approaches that later presented semi-supervised variants that do not require the generation of pseudo-labels. For example: Support Vector Machines [47] (SVM) and Optimum Path Forest [48] (OPF).

The taxonomy and categories of semi-supervised approaches vary in the literature [43], [44]. Generally, there is some overlap among categories. In the following subsections, we present them according to 4 research directions [44]: category regularization; stronger augmentation; convergence with self-supervised learning; and graph-based approaches.

### A. Consistency regularization

These methods rely on a concept known as category regularization. The central idea is to force the approach to produce similar results for augmented versions of the same unlabeled image. This is generally done by considering an additional term in the loss function. The first method as far as it is known, to use this concept is called II-Model [49]. In II-Model, they use translation and random horizontal flips as augmentations for unlabeled data, which is often called weak augmentation.

However, the main issue with II-Model is the unstable target, which compromises the algorithm learning procedure. The Mean Teacher [50] approach was proposed with the intent to address this issue. For this, they use two separate models: the Student network and the Teacher network. While

the Student is trained as usual, the Teacher does not use back-propagation and the weights are updated at each iteration using the weights from the Student network.

### B. Stronger Augmentation

Data augmentation is of crucial importance for various semi-supervised approaches [44]. Some strategies focus on improving the performance of classification by employing different kinds of data augmentation techniques, in such a way that the inputs given to the two branches of the neural model (or, to the two separate networks) are sufficiently distinct. There are many methods that fit in this category, among them: Virtual Adversarial Training and Entropy Minimisation [51] (VAT), Unsupervised Data Augmentation [52] (UDA), MixMatch [53], FixMatch [54], ReMixMatch [55], AlphaMatch [56]. Some of them also mix other ideas, such as the concept of consistency regularization.

### C. Convergence with Self-supervised Learning

Recently, self-supervision has been used by several semi-supervised methods. Self-supervised approaches are a category of representation learning algorithms capable of generating supervision signals without any human annotations. Most approaches in this category use self-supervision to generate a set of pseudo-labels for training. Among the main approaches in this category, we can cite: SimCLR [57], CoMatch [58], Self-Match [59].

### D. Graph-based Approaches

A promising research direction is methods based on graphs. There are different traditional graph-based approaches, both transductive, and inductive ones [43]. The idea is that the elements of the dataset can be represented as nodes and the edges can be used to propagate or represent some kind of information between these nodes. Graph-based methods are usually based on the manifold assumption [43]: the graphs, constructed based on the local similarity between data points, provide a lower-dimensional representation of the potentially high-dimensional input data. This makes these approaches advantageous for scenarios with data of high dimensionality.

Recently, Graph Convolutional Networks (GCN), have been proposed for semi-supervision. While CNNs are specially built to operate on regular (Euclidean) structured data, the GNNs work on graphs with different numbers of vertices and unordered nodes (irregular on non-Euclidean structured data). There are many variants of GCNs proposed: GCN-Net [24], GCN-SGC [29], GCN-GAT [28], GCN-APPNP [30], GCN-ARMA [31]. Also, variants of GNNs: GNN-LDS [34], GNN-KNN-LDS [34].

The GCNs exploit feature vectors and graph-based neighborhood structures to learn more effective representations. Due to these aspects, the GCNs have been recently applied to graph-based data on semi-supervised learning tasks, achieving state-of-the-art results. Several GCN variations have been proposed with relevant results [28]–[31]. The use of GCN has many different applications. There are some recent works that

exploit graph learning for question and answer systems [32], including conversational image search [33].

However, there are still not many approaches for using GCNs in image classification. Among the multiple research topics, there is finding the best approach to model the graph and the features, which are provided as the input for these networks and directly impact their performance and results.

## III. GRAPH-BASED SEMI-SUPERVISED LEARNING FORMULATION

In this section, we first discuss a formal definition of the semi-supervised learning setting for classification tasks using GCNs, mostly following the notation from [24], [60].

Let  $\mathcal{C}=\{o_1, o_2, \dots, o_n\}$  be an object collection, where  $o_i \in \mathcal{C}$  denotes an image and  $n$  denotes the collection size. The collection is represented by an undirected graph  $\mathcal{G}$ . The graph can be formally defined as tuple  $\mathcal{G} = (\mathcal{V}, \mathbf{X}, \mathcal{E})$ , where  $\mathcal{V}$  denotes the node set,  $\mathbf{X}$  is a feature matrix, and  $\mathcal{E}$  denotes the edge set.

The node set is defined by  $\mathcal{V} = \{v_1, v_2, \dots, v_n\}$  where each node  $v_i \in \mathcal{V}$  represents an image  $o_i \in \mathcal{C}$ . Labels can be assigned to nodes  $v_i \in \mathcal{V}$ , such that a set of labels can be defined as  $\mathcal{Y} = \{y_1, y_2, \dots, y_c\}$ . According to the labels, the node set can be more specifically defined as  $\mathcal{V} = \{v_1, v_2, \dots, v_L, v_{L+1}, \dots, v_n\}$ , which denotes a partially labeled data set, where  $\mathcal{V}_L = \{v_i\}_{i=1}^L$  is the labeled data items subset and  $\mathcal{V}_U = \{v_i\}_{i=L+1}^n$  is the unlabeled data items subset. Formally, the training set can be seen as a labeling function  $f_l : \mathcal{V}_L \rightarrow \mathcal{Y}$ , where  $y_i = f_l(v_i) \forall v_i \in \mathcal{V}_L$ . In general, on semi-supervised scenarios, we have  $|\mathcal{V}_L| \ll |\mathcal{V}_U|$ .

The feature matrix can be defined as  $\mathbf{X} = [\mathbf{x}_1, \mathbf{x}_2, \dots, \mathbf{x}_n]^T \in \mathbb{R}^{n \times d}$ , where  $\mathbf{x}_i$  is a  $d$ -dimensional feature vector which represents the image  $o_i$ , or equivalently, the node  $v_i$ . The vector  $\mathbf{x}_i$  is obtained by a feature extraction approach, which can be defined as function  $f_e : \mathcal{C} \rightarrow \mathbb{R}^d$ , such that  $\mathbf{x}_i = f_e(o_i)$ .

The edge set  $\mathcal{E}$  is a set of nodes pairs  $(v_i, v_j)$ , formally defined as  $\mathcal{E} \subseteq \{(v_i, v_j) | (v_i, v_j) \in \mathcal{V}^2 \wedge v_i \neq v_j\}$ . For graph-structured content, the set  $\mathcal{E}$  is intrinsically defined by the data. For general image data, we propose to define the set  $\mathcal{E}$  based on the feature matrix  $\mathbf{X}$ . How to define an effective graph is a central challenge addressed by our approach, discussed in the next section.

Once defined the graph  $\mathcal{G}$ , a GCN model denoted by a function  $f_{gcn}$  can be used to learn an embedded representation  $\mathbf{z}_i$  for each node  $v_i$ . The learned representation is exploited to perform classification tasks. Formally, the classification goal is to learn a function  $\hat{f}_l : \mathcal{V}_U \rightarrow \mathcal{Y}$  to predict the labels of unlabeled nodes in  $\mathcal{V}_U$ .

## IV. MANIFOLD-BASED GRAPH CONVOLUTIONAL NETWORK

In this work, we propose the Manifold-based Graph Convolutional Network (Manifold-GCN), a semi-supervised framework based on the use of manifold learning and GCN models for image classification for scenarios with limited labeled data. The initial representations were obtained by deep features

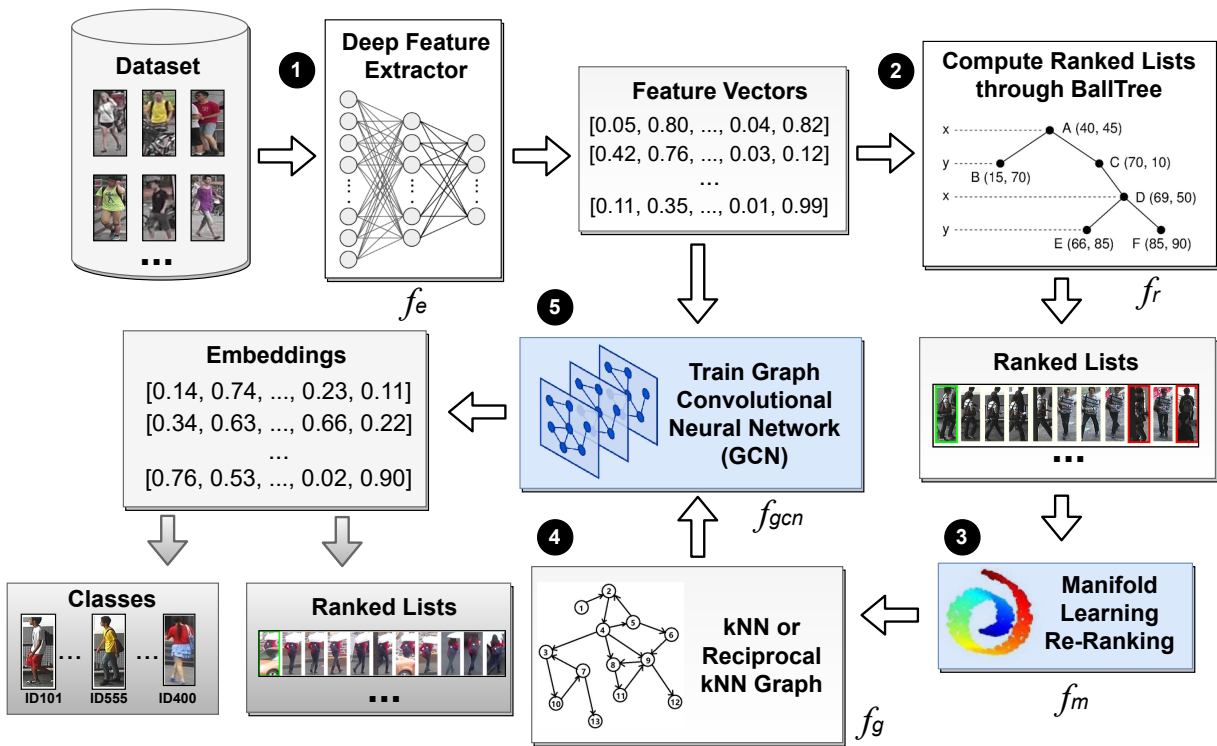


Fig. 1: Workflow of our proposed Manifold-GCN framework for image classification. The steps of the approach are numbered.

extracted by CNN and ViT models trained on a transfer learning setting. Given the representations, the central idea consists in exploiting contextual similarity measures given by unsupervised manifold learning methods for computing a graph. The similarity information encoded in the graph is exploited by GCN models for learning novel representations used for classification.

Figure 1 illustrates the main steps that compose our strategy. Each step is identified by a number (top of boxes) and a function (bottom of boxes). In **(1)**, a feature vector is extracted for representing each image. In **(2)**, representations are processed in order to obtain ranked lists, which encode the similarity information. Unsupervised manifold learning methods are used to analyze contextual similarity information and compute more effective rankings in **(3)**. In **(4)**, the outputs of the manifold learning methods are modeled as kNN graphs or reciprocal kNN graphs. In **(5)**, the graph and features are jointly provided to the GCN models for semi-supervised training. The embeddings obtained for each of the elements of the dataset can be used for classification, through a softmax operation. Each of the main steps of the framework is described in the next subsections.

#### A. Similarity Measurement and Ranking Model

In the proposed approach, the similarity information is encoded on ranking structures. Let us consider a ranking task in which, given a query image, an ordered list of images from the collection is returned according to the similarity to the query. Formally, given a query image  $o_q$ , a ranked list  $\tau_q = (o_1, o_2, \dots, o_L)$  in response to the query, where  $L$  denotes the length of the list. The ranked list  $\tau_q$  can be defined as a

permutation of a set  $\mathcal{C}_L$  which contains the  $L$  most similar images to image  $x_q$  in the collection  $\mathcal{C}$ . The permutation  $\tau_q$  is a bijection from the set  $\mathcal{C}_L$  onto the set  $[L] = \{1, 2, \dots, L\}$ . The  $\tau_q(o_i)$  notation denotes the position (or rank) of image  $o_i$  in the ranked list  $\tau_q$ .

The ranked list  $\tau_q$  can be computed based on the comparison between image representations. Let  $d: \mathbb{R}^d \times \mathbb{R}^d \rightarrow \mathbb{R}$  be a distance function that computes the distance between two images according to their corresponding feature vectors. The Euclidean distance is often used as the distance function. Formally, the distance between two images  $o_i, o_j$  is defined by  $d(\mathbf{x}_i, \mathbf{x}_j)$ .

For a given query, a ranked list can be obtained by sorting images in increasing order of the distance. In terms of ranking positions, we can say that if image  $o_i$  is ranked before image  $o_j$  in the ranked list of image  $o_q$ , that is,  $\tau_q(o_i) < \tau_q(o_j)$ , then  $d(\mathbf{x}_q, \mathbf{x}_i) \leq d(\mathbf{x}_q, \mathbf{x}_j)$ . Taking every image in the collection as a query image  $x_q$ , a set of ranked lists  $\mathcal{T} = \{\tau_1, \tau_2, \dots, \tau_n\}$  can be obtained. In this way, the set  $\mathcal{T}$  can be obtained from the feature matrix  $\mathbf{X}$  and the ranking task defined by a function  $f_r$ , such that  $\mathcal{T} = f_r(\mathbf{X})$ . Tree-based indexing structures [61] and hashing approaches [62] can be exploited in order to provide efficient implementations for the function  $f_r$ . In this work, we consider BallTree [61], [63] structures.

#### B. Unsupervised Manifold Learning

How to accurately define distance or similarity among data elements is a challenging and fundamental step in many machine learning tasks. The most common approach is given by pairwise comparisons based on Euclidean-like distance

functions. However, pairwise analyses ignore contextual information and complex similarity arrangements encoded in the structural information of the dataset manifold. Aiming at addressing such drawbacks, many contextual similarity approaches take into account the structure of datasets in order to compute more global and effective similarity measures.

Manifold Learning is a wide term that has many different definitions in the literature. In general, manifold Learning approaches aim to capture and exploit the intrinsic manifold structure to compute a more effective distance/similarity measure [42]. Recently, unsupervised manifold learning approaches based on ranking information have achieved relevant advances in contextual similarity measurement [19], [20], [64].

In fact, the set of ranked lists  $\mathcal{T}$  encodes rich similarity information about the image collection. The main objective of rank-based manifold learning methods is to exploit such information to capture the structure of the dataset manifold. Therefore, this step consists of the use of unsupervised manifold learning methods for processing the original ranked lists, providing more effective ranking results which are subsequently modeled as graphs to be submitted to a GCN model.

Formally, the manifold learning methods can be defined as a function  $f_m$  that receives a set of ranked lists  $\mathcal{T}$  as input and returns a set of ranked lists  $\mathcal{T}_m$  as output, which is expected to be more effective than the original:

$$\mathcal{T}_m = f_m(\mathcal{T}). \quad (1)$$

Once defined under a common formulation, three different manifold learning algorithms were considered to instantiate the proposed approach (described in Section V).

### C. Graph Building

The improved set of ranked lists computed by the manifold learning methods is used to build a graph. The motivation is based on the conjecture that more effective similarity information can be extracted and encoded in the graph by exploiting the processed ranked lists. Let  $\mathcal{G} = (\mathcal{V}, \mathbf{X}, \mathcal{E})$  be the graph defined in Section III. We propose to compute the edge set  $\mathcal{E}$  as a function of the set of ranked lists  $\mathcal{T}_m$ , such that  $\mathcal{E} = f_g(\mathcal{T}_m)$ .

This work considers two distinct approaches to define the function  $f_g$ . The similarity information encoded in the ranked lists is modeled through different neighborhood set formulations. Both approaches are discussed in the following.

- *Traditional kNN Graph:* the kNN graph is based on the natural neighborhood set. Given an element  $o_q$ , the natural neighborhood set  $\mathcal{N}(o_q, k)$  contains the  $k$  most similar elements to  $o_q$ , which can be formally defined as:

$$\mathcal{N}(o_q, k) = \{\mathcal{X} \subseteq \mathcal{C}, |\mathcal{X}| = k \wedge \forall o_i \in \mathcal{X}, o_j \in \mathcal{C} - \mathcal{X} : \tau_q(o_i) < \tau_q(o_j)\}. \quad (2)$$

Therefore, the edge set  $\mathcal{E}$  of the kNN graph can be defined as:

$$\mathcal{E} = \{(o_q, o_j) \mid o_j \in \mathcal{N}(o_q, k)\}. \quad (3)$$

In other words, each element has an edge to the  $k$  most similar elements.

- *Reciprocal kNN Graph:* the reciprocal kNN graph is based on the reciprocal neighborhood set [65], which requires a stronger bidirectional similarity relationship. Different from the natural neighborhood set, which is not symmetrical, the reciprocal neighborhood set is symmetrically defined as:

$$\mathcal{N}_r(o_q, k) = \{obj_i \mid obj_i \in \mathcal{N}(o_q, k) \wedge o_q \in \mathcal{N}(o_i, k)\}. \quad (4)$$

The edge set  $E$  for the reciprocal kNN set can be defined as:

$$\mathcal{E} = \{(o_q, o_j) \mid o_j \in \mathcal{N}_r(o_q, k)\}. \quad (5)$$

Thus, we can interpret that there are edges between the elements  $o_q$  and  $o_j$  if they are reciprocal neighbors in the top- $k$  positions of their ranked lists.

For both kNN and reciprocal kNN approaches, the edge set  $\mathcal{E}$  can be represented by a non-negative adjacency matrix  $\mathbf{A} = [a_{ij}] \in \mathbb{R}^{n \times n}$ , which can be defined as:

$$a_{ij} = \begin{cases} 1, & (o_i, o_j) \in \mathcal{E} \\ 0, & \text{otherwise.} \end{cases} \quad (6)$$

The adjacency matrix  $\mathbf{A}$  is used as input by GCN models, as discussed in next section.

### D. Graph Convolutional Networks

Graph Convolutional Networks (GCN), originally introduced in [24], aim at learning novel and more effective representations (embeddings) for each graph node. It is done by iteratively aggregating the embeddings of its neighbors, encoding the graph structure directly in a neural network model. The original model proposed in [24] is a two-layer GCN model which uses the graph represented by the adjacency matrix  $\mathbf{A}$  for semi-supervised node classification.

The network model can be depicted as a function both on the feature data  $\mathbf{X}$  and on the adjacency matrix  $\mathbf{A}$ , as:

$$\mathbf{Z} = f_{gcn}(\mathbf{X}, \mathbf{A}), \quad (7)$$

where  $\mathbf{Z}$  denotes an embedding matrix, such that  $\mathbf{Z} = [\mathbf{z}_1, \mathbf{z}_2, \dots, \mathbf{z}_n]^T \in \mathbb{R}^{n \times c}$  and  $\mathbf{z}_i$  is a  $c$ -dimensional embedded representation learned for the node  $v_i$ ; where  $n$  is the dataset size and  $c$  corresponds to the number of classes.

The degree matrices are computed as a pre-processing step, defined as  $\hat{\mathbf{A}} = \tilde{\mathbf{D}}^{-1/2} \tilde{\mathbf{A}} \tilde{\mathbf{D}}^{-1/2}$ , where  $\tilde{\mathbf{A}} = \mathbf{A} + \mathbf{I}$  and  $\tilde{\mathbf{D}}$  is the degree matrix of  $\tilde{\mathbf{A}}$ . Then, the function  $f_{gcn}(\cdot)$  which represents the two-layer GCN model assumes the form:

$$\mathbf{Z} = f(\mathbf{X}, \mathbf{A}) = \text{softmax}(\hat{\mathbf{A}} \text{ReLU}(\hat{\mathbf{A}} \mathbf{X} \mathbf{W}^{(0)}) \mathbf{W}^{(1)}). \quad (8)$$

The matrix  $\mathbf{W}^{(0)} \in \mathbb{R}^{d \times H}$  defines the neural network weights for an input-to-hidden layer with  $H$  feature maps, while  $\mathbf{W}^{(1)} \in \mathbb{R}^{H \times c}$  is a hidden-to-output matrix. Both matrices  $\mathbf{W}^{(0)}$  and  $\mathbf{W}^{(1)}$  are trained using gradient descent, considering the cross-entropy error over all labeled nodes.  $v_i \in \mathcal{V}_L$ .

The activation function is applied row-wise and is defined as  $\text{softmax}(z_i) = \frac{\exp(z_i)}{\sum_i \exp(z_i)}$ , where  $z_i$  is the position  $i$  of embedding  $\mathbf{z}_i$ .

The softmax yields the probability distribution over the  $c$  class labels for each row, i.e., the probability values sum up to 1 for each row. Given an image  $o_i$ , the learned embedded representation  $\mathbf{z}_i$  is then used for classification tasks by applying an argmax over the output of the softmax.

## V. GCNS AND MANIFOLD LEARNING METHODS

The proposed approach is flexible in the sense that it can be instantiated by different GCN models and manifold learning methods. This section briefly describes the GCN models and the manifold learning methods considered in this work.

### A. GCN Models

The original GCN [24] model and more 4 variants [29]–[31] are used in the proposed Manifold-GCN approach. The GCN models employed are:

- **Graph Convolution Network (GCN)** [24]: the first GCN proposed, introducing the idea of convolutions applied to graph domains, often known as GCN-Net or simply GCN;
- **Simple Graph Convolution (SGC)** [29]: a simplification of the conventional GCN models which removes the nonlinearities and collapses weight matrix between consecutive layers;
- **Graph Attention Networks (GAT)** [28]: employs auto-attention layers with the idea of solving the main shortcomings of the previous GCN models. The layers are stacked in a way that it is possible to specify different weights for nodes of the same neighborhood without requiring costly operations;
- **Approximate Personalized Propagation of Neural Predictions (APNP)** [30]: a model that combines a GCN with the PageRank algorithm, deriving a propagation strategy based on a modified PageRank approach;
- **Auto-Regressive Moving Average (ARMA) Filter Convolution** [31]: a GCN variant that defines convolutional layers based on filters of Auto-Regressive Moving Average type.

### B. Manifold Learning Methods

Manifold learning can be broadly understood as the process of non-linear dimensionality reduction by performing distance learning for a set of features. In fact, images are commonly represented as points in a high-dimensional feature space. However, it has been shown that data samples often live in a much lower dimensional intrinsic space [42]. Therefore, how to capture and exploit the intrinsic manifold structure to compute a more effective distance/similarity measure becomes a key task in many areas [42]. In this work, we consider recent unsupervised manifold learning methods to provide more effective similarity measures using rank-based approaches. Three of them are considered:

- **Log-based Hypergraph of Ranking References (LHRR)** [19]: an algorithm that models the input ranked

lists as hypergraphs and exploits the relations between the elements in the dataset.

- **BFS-Tree of Ranking References (BFSTREE)** [64]: it uses a breadth-first tree structure that models the similarity information between the elements in the ranked lists, which is employed with the objective of analyzing the implicit relations between the elements of the dataset. The tree structure allows a representation of the top- $k$  elements such that the weights of the edges are computed based on the correlations among the ranked lists.
- **The Rank-based Diffusion Process with Assured Convergence (RDPAC)** [20]: it performs a diffusion process to exploit the information contained in the ranked lists. It also presents formal proof for the convergence of the diffusion process. The asymptotic complexity of the algorithm is low, which allows its use in many different scenarios with a great number of data elements.

## VI. EXPERIMENTAL EVALUATION

This section discusses the experimental evaluation conducted to assess the effectiveness of the proposed Manifold-GCN. Section VI-A describes the datasets and features considered. Section VI-B discusses the experimental protocol. The semi-supervised image classification results are presented in Section VI-C. Section VI-D shows visualizations of feature space improvements, while Section VI-E reports a comparison with both traditional and recent state-of-the-art methods, Section VI-F reports the run-time for each step of the proposed approach.

### A. Datasets and Features

Three public datasets were considered in the experimental evaluation:

- **Flowers17** [66]: traditional dataset composed of 1,360 images of 17 species of flowers;
- **Corel5k** [67]: 5,000 diverse images (cars, animals, buildings, and others) divided into 100 classes;
- **CUB-200-2011** [68]: a popular benchmark for image classification composed by 11,788 photos of 200 bird species;

A diverse set of deep features was considered in the conducted experiments. For the general purpose datasets (Flowers17, Corel5k, and CUB-200-2011), all CNNs were trained on ImageNet [69] dataset through. The extractions were performed with the PyTorch framework<sup>1</sup>. In all cases, the Euclidean distance was considered.

We also employ two different types of Vision Transformers: An Image is Worth 16x16 Words Visual Transformer (ViT-B/16) [70]<sup>2</sup> and Tokens-To-Token Vision Transformer (T2T-ViT) [71]<sup>3</sup>. Both were trained on ImageNet [69] dataset.

<sup>1</sup><https://github.com/Cadene/pretrained-models.pytorch>

<sup>2</sup><https://github.com/faustomorales/vit-keras>

<sup>3</sup><https://github.com/yitu-opensource/T2T-ViT>

## B. Experimental Protocol

In this work, the training data is the labeled set and the testing data is the unlabeled set. The unlabeled data considered during the training process comes from the test set. This protocol was also adopted for all baselines.

For the manifold learning approach, all the data is used for the distance learning process, which is completely unsupervised; no labels are used. In the second step, the semi-supervised classification by the GCN, we perform cross-validation that, in our case, consists of a 10-fold split where one fold is used for training and the rest is used for testing. For each of 10 executions (one for every fold being considered as training) and 90% is considered as testing data (unlabeled data). We highlight that, since we are running 10 executions by changing the folds, every dataset element will be considered as training or test at least once. Therefore, each reported value corresponds to the mean of 50 executions (number of executions multiplied by the number of folds).

For all the GCNs, the Adam optimizer with a learning rate of  $10^{-5}$  was used, except for Cub200, in which we used a learning rate of  $10^{-4}$ . Regarding the number of neurons, we used 256. The only exceptions are GCN-SGC, which does not have this parameter; and GCN-GAT which has a number of heads, which was set to 32. The training processes consisted of 200 epochs, using input graphs with  $k = 40$ . In the same way, the manifold learning methods also have a parameter  $k$ , which is different from the graph  $k$ . For the method  $k$ , we also used  $k = 40$ .

## C. Classification Results

The proposed approach was evaluated on a wide diversity of semi-supervised classification scenarios, considering 3 distinct datasets (Flowers, Corel5k, and CUB200). For each dataset, 4 to 5 deep learning features trained on a transfer learning setting were used, considering both CNNs and Vision Transformers approaches. For classification, 5 GCNs models are evaluated considering both the traditional and reciprocal kNN graphs. The impact of re-ranking step is also assessed, evaluating the classification results with and without this step, considering 3 distinct rank-based manifold learning methods. In the semi-supervised scenario, the mean of 5 executions for 10 folds was performed.

Tables I, II and III present the results for the datasets Flowers, Corel5k, and CUB200, respectively. The best result for each feature/GCN is highlighted in bold. The gray highlight is used to indicate the best result for the corresponding GCN. The blue color indicates the best result for the dataset (the best result in the whole table).

Some interesting observations can be made from the experimental results. In general, it can be noticed that the reciprocal kNN graph outperforms the traditional kNN graph. It can be observed that the use of manifold learning methods outperforms the scenarios without its use. Moreover, the combination of reciprocal kNN graph and manifold learning methods leads to the best results for all GCN models (gray highlight) and datasets (in blue).

Among the features, VIT-B16 yielded the best results. Therefore, there is a correlation that shows that the better the feature, the better the classification result. In this case, the best feature is VIT-B16. For GCN models and manifold learning methods, the diversity is higher, but GCN-SGC and RDPAC achieved the best results in most of the scenarios. We also can highlight the remarkable gains obtained on all datasets and features from the original (kNN without re-ranking) to the proposed approach (reciprocal kNN with re-ranking). For CUB200, the most challenging dataset, the accuracy of GCN-APPNP was improved from 55.24% to 75.59%.

Our method was also evaluated considering the weighted F-Measure. Figure 2 reports the results for GCN-SGC on the traditional kNN graph (on the left) and the Reciprocal kNN graph (on the right). For every graph, we see that using manifold learning improves the results of the traditional GCN.

## D. Visualization Results

In order to visualize the effectiveness of our approach, an experiment was conducted showing the distribution of features in a 2D space, after being processed by t-Distributed Stochastic Neighbor Embedding (TSNE) [72]. Figure 3 shows the results for (a) the original CNN-ResNet features; (b) the GCN output with kNN graph; (c) the GCN output with kNN graph and manifold learning; (d) the GCN output with Reciprocal graph and manifold learning. The Flowers-17 was chosen for this visualization due to the small number of classes, which makes it easier to visualize the improvements. Each class is represented by a different combination of shape and color. Notice that the distribution of classes is further improved when the Manifold-GCN is applied (c and d), which is consistent with our main hypothesis.

## E. Comparison with Other Approaches

For comparison purposes, a wide variety of supervised and semi-supervised classification approaches were considered, both traditional and more recent ones. A brief description of the employed baselines, the implementations, and the parameters used are presented in the following:

- **$k$  Nearest Neighbor (kNN)**: traditional approach that computes the distance to the other elements in the dataset and selects the  $k$  closest ones. The sklearn implementation was used, with  $k = 20$ .
- **Support Vector Machine (SVM)** [47]: it is a traditional method that consists in finding the hyperplane that best separates the data into the correct classes in a high-dimensional space. The sklearn implementation was used, with default parameters and Radial Basis Function (RBF) kernel.
- **Single-Layer and Multi-Layer Perceptron**: the sklearn implementation was used for both, with the Stochastic Gradient Descent (SGD) optimizer.
- **Optimum-Path Forest (OPF)** [48], [75]: it builds a graph where each node is an element of the dataset and the edges are weighted by their Euclidean distance. The algorithm computes the optimum path between the nodes

TABLE I: Impact of manifold learning approaches (LHRR, RDPAC, BFSTREE) and Reciprocal Graph (Rec.) on the classification accuracy (%) of 5 different GCN models on Flowers17 dataset. The best results for each feature and GCN model are highlighted in bold, the best results for each GCN model are marked with a gray background, and the best result for the entire dataset is highlighted in blue. In all the cases, the best results used manifold learning and Reciprocal Graph.

Classifier Specification			Feature				
GCN	Graph	Re-Rank	CNN-ResNet [9]	CNN-DPNet [10]	CNN-SENet [73]	T2T-VIT24 [71]	VIT-B16 [70]
GCN-Net	kNN	—	79.08 ± 0.3039	76.94 ± 0.3688	72.72 ± 0.2052	69.75 ± 0.0827	92.72 ± 0.1324
	kNN	LHRR	84.37 ± 0.3239	80.76 ± 0.1372	73.89 ± 0.133	72.03 ± 0.1131	95.88 ± 0.0567
	kNN	RDPAC	83.91 ± 0.1279	81.24 ± 0.2597	74.76 ± 0.2245	74.60 ± 0.1353	96.86 ± 0.0702
	kNN	BFSTREE	83.12 ± 0.1784	81.39 ± 0.1222	74.83 ± 0.1284	72.49 ± 0.3283	96.33 ± 0.0695
	Rec.	—	83.89 ± 0.1973	81.19 ± 0.264	76.23 ± 0.1913	75.82 ± 0.2096	97.07 ± 0.0606
	Rec.	LHRR	<b>84.67 ± 0.0988</b>	80.64 ± 0.1749	73.97 ± 0.1383	72.40 ± 0.1927	95.39 ± 0.1583
	Rec.	RDPAC	84.20 ± 0.1975	<b>82.27 ± 0.1659</b>	<b>76.61 ± 0.1968</b>	<b>75.87 ± 0.1877</b>	<b>97.16 ± 0.0168</b>
	Rec.	BFSTREE	82.97 ± 0.1623	81.20 ± 0.1141	74.80 ± 0.2034	73.26 ± 0.1008	96.52 ± 0.0538
GCN-SGC	kNN	—	79.64 ± 0.1023	77.09 ± 0.1139	73.00 ± 0.0941	70.05 ± 0.0802	92.84 ± 0.0655
	kNN	LHRR	84.41 ± 0.0835	80.36 ± 0.0661	74.04 ± 0.0599	72.11 ± 0.113	95.85 ± 0.0285
	kNN	RDPAC	84.19 ± 0.0659	81.12 ± 0.0645	75.06 ± 0.0627	75.18 ± 0.0743	96.95 ± 0.0133
	kNN	BFSTREE	83.33 ± 0.0533	81.54 ± 0.0410	75.08 ± 0.0565	72.86 ± 0.0879	96.42 ± 0.0396
	Rec.	—	83.99 ± 0.0478	81.32 ± 0.0314	76.16 ± 0.0415	75.69 ± 0.0828	96.93 ± 0.0464
	Rec.	LHRR	<b>84.91 ± 0.0665</b>	80.75 ± 0.0694	74.60 ± 0.0510	72.95 ± 0.0563	95.47 ± 0.0171
	Rec.	RDPAC	84.53 ± 0.0580	<b>82.53 ± 0.1335</b>	<b>76.93 ± 0.0376</b>	<b>76.43 ± 0.0499</b>	<b>97.11 ± 0.0163</b>
	Rec.	BFSTREE	83.43 ± 0.0200	81.58 ± 0.1169	75.03 ± 0.0313	73.58 ± 0.026	96.63 ± 0.0337
GCN-GAT	kNN	—	80.67 ± 0.2144	65.60 ± 0.9961	74.64 ± 0.3048	67.33 ± 0.9069	93.65 ± 0.228
	kNN	LHRR	84.52 ± 0.3202	76.15 ± 1.4547	75.48 ± 0.2365	73.37 ± 0.2824	95.33 ± 0.2522
	kNN	RDPAC	84.02 ± 0.1058	77.39 ± 1.2703	75.29 ± 0.3550	75.40 ± 0.4316	97.09 ± 0.0572
	kNN	BFSTREE	83.04 ± 0.1844	77.19 ± 1.833	75.82 ± 0.2086	73.26 ± 0.3184	96.41 ± 0.0465
	Rec.	—	83.67 ± 0.1965	77.42 ± 0.6762	76.74 ± 0.3398	74.82 ± 0.2978	96.99 ± 0.0558
	Rec.	LHRR	<b>84.82 ± 0.2194</b>	79.63 ± 0.6337	75.22 ± 0.2648	73.32 ± 0.3684	95.21 ± 0.2575
	Rec.	RDPAC	84.40 ± 0.1488	<b>79.69 ± 1.0373</b>	<b>77.18 ± 0.2940</b>	<b>76.90 ± 0.3418</b>	<b>97.22 ± 0.0557</b>
	Rec.	BFSTREE	82.79 ± 0.2926	78.74 ± 0.2682	75.94 ± 0.2681	73.85 ± 0.2632	96.55 ± 0.0881
GCN-APPNP	kNN	—	77.25 ± 0.1692	76.38 ± 0.238	71.0 ± 0.4051	69.45 ± 0.3072	90.24 ± 0.2128
	kNN	LHRR	84.58 ± 0.2621	82.53 ± 0.2443	76.83 ± 0.1622	74.32 ± 0.2989	96.05 ± 0.0421
	kNN	RDPAC	85.35 ± 0.2205	83.32 ± 0.1287	76.89 ± 0.3673	77.87 ± 0.0660	97.28 ± 0.0303
	kNN	BFSTREE	84.22 ± 0.1638	83.34 ± 0.0875	77.94 ± 0.3084	75.65 ± 0.2505	96.73 ± 0.0763
	Rec.	—	83.91 ± 0.1181	82.20 ± 0.2160	77.74 ± 0.1645	77.11 ± 0.1485	97.24 ± 0.0470
	Rec.	LHRR	<b>85.88 ± 0.1896</b>	82.55 ± 0.2138	76.60 ± 0.2479	75.40 ± 0.2458	95.68 ± 0.1083
	Rec.	RDPAC	85.41 ± 0.2304	<b>83.99 ± 0.1276</b>	<b>78.82 ± 0.1466</b>	<b>78.01 ± 0.1307</b>	<b>97.43 ± 0.0699</b>
	Rec.	BFSTREE	83.75 ± 0.2099	83.14 ± 0.1915	77.83 ± 0.1826	75.85 ± 0.2098	96.89 ± 0.0632
GCN-ARMA	kNN	—	78.69 ± 0.2471	76.01 ± 0.295	73.18 ± 0.4015	70.47 ± 0.2548	91.27 ± 0.1731
	kNN	LHRR	84.64 ± 0.3211	81.90 ± 0.4272	76.09 ± 0.1451	74.26 ± 0.2543	95.66 ± 0.1726
	kNN	RDPAC	85.05 ± 0.1643	82.38 ± 0.3741	76.18 ± 0.3637	76.75 ± 0.2599	96.88 ± 0.0698
	kNN	BFSTREE	83.72 ± 0.0791	81.96 ± 0.3477	76.81 ± 0.1272	75.03 ± 0.1647	96.24 ± 0.0812
	Rec.	—	83.32 ± 0.3713	80.86 ± 0.1282	76.96 ± 0.3041	76.11 ± 0.3851	96.66 ± 0.1140
	Rec.	LHRR	<b>85.36 ± 0.3818</b>	82.17 ± 0.3283	75.92 ± 0.2516	74.64 ± 0.3728	95.13 ± 0.2118
	Rec.	RDPAC	84.97 ± 0.2524	<b>83.14 ± 0.3078</b>	<b>77.89 ± 0.2358</b>	<b>77.81 ± 0.3271</b>	<b>97.02 ± 0.0944</b>
	Rec.	BFSTREE	84.06 ± 0.2612	82.21 ± 0.1901	76.88 ± 0.1897	75.10 ± 0.3000	96.47 ± 0.1171

in order to classify them into a given class. The pyOPF<sup>4</sup> implementation was used, with the default parameters.

- **Pseudo-label** [46]: the method is semi-supervised and is used to assign labels to unlabeled data. In this work, a public implementation<sup>5</sup> was used along with the Logistic Regression classifier that employed the Stochastic Gradient Descent (SGD) optimizer and Squared Hinge loss with  $\alpha = 10^{-5}$  for training.
- **Label Spreading (LS)** [45]: a semi-supervised algorithm that attributes labels to elements according to the labels of their neighbors, given a certain degree of similarity. For this process, it uses an affinity matrix based on a

normalized graph Laplacian. The sklearn implementation was used, considering a Radial Basis Function (RBF) kernel with  $\alpha = 0.4125$ ,  $\gamma = 0.1$ , and a maximum of 100 iterations. This method is used to expand the training set and is used along with the other classifiers.

- **Learning Discrete Structures for Graph Neural Networks (GNN-LDS and GNN-KNN-LDS)** [34]: this Graph Neural Network (GNN) learns both a graph and embeddings from the input features. It approximately solves a bilevel program that learns a discrete probability distribution on the edges of the graph. The authors claim that this is the first method that simultaneously learns the graph and the parameters of a GNN for semi-supervised classification. The approach presents two variants: (i) GNN-LDS; and (ii) GNN-KNN-LDS which initializes by

<sup>4</sup><https://github.com/marcoscleison/PyOPF>

<sup>5</sup>[https://github.com/anirudhshenoy/pseudo\\_labeling\\_small\\_datasets](https://github.com/anirudhshenoy/pseudo_labeling_small_datasets)

TABLE II: Impact of manifold learning approaches (LHRR, RDPAC, BFSTREE) and Reciprocal Graph (Rec.) on the classification accuracy (%) of 5 different GCN models on Core15k dataset. The best results for each feature and GCN model are highlighted in bold, the best results for each GCN model are marked with a gray background, and the best result for the entire dataset is highlighted in blue. In all the cases, the best results used manifold learning.

Classifier Specification			Feature				
GCN	Graph	Re-Rank	CNN-ResNet [9]	CNN-DPNet [10]	CNN-SENet [73]	T2T-VIT24 [71]	VIT-B16 [70]
GCN-Net	kNN	—	89.34 ± 0.0950	86.49 ± 0.0998	89.17 ± 0.0956	89.02 ± 0.1452	89.93 ± 0.2878
	kNN	LHRR	91.40 ± 0.0906	88.94 ± 0.1958	90.19 ± 0.1392	90.68 ± 0.0957	94.57 ± 0.121
	kNN	RDPAC	91.46 ± 0.1402	89.05 ± 0.1054	90.65 ± 0.0483	91.77 ± 0.1246	94.29 ± 0.139
	kNN	BFSTREE	<b>92.03 ± 0.1165</b>	89.28 ± 0.1858	91.19 ± 0.1102	91.78 ± 0.0432	94.30 ± 0.3362
	Rec.	—	91.68 ± 0.1064	<b>89.62 ± 0.1114</b>	<b>91.81 ± 0.1159</b>	92.19 ± 0.0908	93.42 ± 0.1987
	Rec.	LHRR	91.68 ± 0.0224	88.48 ± 0.1268	90.58 ± 0.0901	91.50 ± 0.0684	94.63 ± 0.139
	Rec.	RDPAC	92.00 ± 0.1434	89.55 ± 0.0944	90.93 ± 0.1654	91.96 ± 0.0705	<b>94.76 ± 0.1577</b>
	Rec.	BFSTREE	92.00 ± 0.0954	89.33 ± 0.1221	91.32 ± 0.0833	<b>92.43 ± 0.0401</b>	94.39 ± 0.2771
GCN-SGC	kNN	—	89.62 ± 0.0321	86.78 ± 0.0256	89.81 ± 0.0426	88.95 ± 0.0482	93.36 ± 0.0401
	kNN	LHRR	91.19 ± 0.0262	88.74 ± 0.0242	89.90 ± 0.044	90.49 ± 0.0518	95.20 ± 0.0219
	kNN	RDPAC	91.47 ± 0.0216	88.95 ± 0.0632	90.70 ± 0.0403	91.77 ± 0.0521	94.76 ± 0.078
	kNN	BFSTREE	91.98 ± 0.0246	89.23 ± 0.0453	91.40 ± 0.0061	91.71 ± 0.0444	95.26 ± 0.0759
	Rec.	—	91.98 ± 0.0133	89.83 ± 0.0415	<b>92.15 ± 0.0164</b>	<b>92.75 ± 0.0908</b>	95.49 ± 0.0107
	Rec.	LHRR	91.73 ± 0.0508	88.70 ± 0.0669	90.73 ± 0.0235	91.68 ± 0.0305	<b>95.57 ± 0.017</b>
	Rec.	RDPAC	92.00 ± 0.0247	<b>89.84 ± 0.1057</b>	90.85 ± 0.0396	92.31 ± 0.072	95.50 ± 0.020
	Rec.	BFSTREE	<b>92.04 ± 0.009</b>	89.49 ± 0.0627	91.30 ± 0.0257	92.54 ± 0.0591	95.30 ± 0.0479
GCN-GAT	kNN	—	90.48 ± 0.1727	83.28 ± 0.33	91.13 ± 0.1107	90.7 ± 0.1187	91.3 ± 0.1764
	kNN	LHRR	92.21 ± 0.1328	88.59 ± 0.4012	91.28 ± 0.2208	92.2 ± 0.0839	94.56 ± 0.1777
	kNN	RDPAC	91.86 ± 0.1403	89.78 ± 0.2723	91.41 ± 0.1429	92.82 ± 0.0956	94.46 ± 0.2555
	kNN	BFSTREE	<b>92.42 ± 0.1008</b>	89.61 ± 0.362	91.95 ± 0.1382	93.09 ± 0.1337	94.58 ± 0.2226
	Rec.	—	92.02 ± 0.0917	89.0 ± 0.2638	<b>92.23 ± 0.0844</b>	92.81 ± 0.113	93.64 ± 0.2373
	Rec.	LHRR	92.19 ± 0.1057	89.17 ± 0.2074	91.18 ± 0.1451	92.41 ± 0.1456	94.55 ± 0.1918
	Rec.	RDPAC	92.22 ± 0.0858	<b>90.48 ± 0.1718</b>	91.48 ± 0.1021	93.02 ± 0.1334	<b>94.89 ± 0.1492</b>
	Rec.	BFSTREE	92.30 ± 0.1128	90.01 ± 0.2374	91.88 ± 0.1081	<b>93.35 ± 0.1537</b>	94.75 ± 0.1385
GCN-APPNP	kNN	—	89.72 ± 0.2031	87.68 ± 0.0785	89.92 ± 0.0992	89.86 ± 0.0731	86.89 ± 0.2487
	kNN	LHRR	92.6 ± 0.0625	90.81 ± 0.1043	91.49 ± 0.1307	91.83 ± 0.0952	94.53 ± 0.1144
	kNN	RDPAC	92.69 ± 0.1161	90.75 ± 0.179	91.81 ± 0.098	92.58 ± 0.0588	94.12 ± 0.2213
	kNN	BFSTREE	93.04 ± 0.0872	<b>91.01 ± 0.1026</b>	92.35 ± 0.0535	92.83 ± 0.031	94.37 ± 0.0855
	Rec.	—	92.69 ± 0.05	90.70 ± 0.1301	<b>92.79 ± 0.0429</b>	93.56 ± 0.0669	93.53 ± 0.1042
	Rec.	LHRR	92.88 ± 0.1058	89.99 ± 0.0869	91.78 ± 0.0694	92.63 ± 0.0817	94.95 ± 0.2116
	Rec.	RDPAC	92.82 ± 0.046	90.95 ± 0.1134	91.92 ± 0.0738	93.17 ± 0.0804	<b>95.13 ± 0.1095</b>
	Rec.	BFSTREE	<b>93.08 ± 0.0727</b>	90.78 ± 0.1317	92.39 ± 0.0269	<b>93.70 ± 0.0653</b>	94.72 ± 0.1564
GCN-ARMA	kNN	—	88.58 ± 0.312	86.47 ± 0.0729	89.11 ± 0.1061	89.16 ± 0.0571	85.48 ± 0.3945
	kNN	LHRR	91.58 ± 0.1185	89.84 ± 0.1565	90.98 ± 0.1738	91.46 ± 0.0963	90.66 ± 0.5051
	kNN	RDPAC	91.72 ± 0.1775	90.09 ± 0.2858	91.08 ± 0.1226	92.28 ± 0.0545	92.62 ± 0.4067
	kNN	BFSTREE	92.23 ± 0.1447	90.31 ± 0.1195	91.7 ± 0.0869	92.24 ± 0.0682	92.28 ± 0.3061
	Rec.	—	91.14 ± 0.137	89.24 ± 0.2139	91.31 ± 0.1887	91.84 ± 0.0774	90.48 ± 0.1707
	Rec.	LHRR	91.77 ± 0.1541	89.24 ± 0.1428	91.07 ± 0.126	91.78 ± 0.1145	92.39 ± 0.2078
	Rec.	RDPAC	92.05 ± 0.1403	<b>90.41 ± 0.1645</b>	91.47 ± 0.1202	92.49 ± 0.2056	92.80 ± 0.1896
	Rec.	BFSTREE	<b>92.27 ± 0.0377</b>	90.14 ± 0.1897	<b>91.71 ± 0.1753</b>	<b>92.90 ± 0.1446</b>	<b>92.74 ± 0.2083</b>

computing a kNN graph. Both were used as baselines with their default parameters proposed in the implementation<sup>6</sup> provided by the original authors. For the kNN graph,  $k = 20$  was used.

- **Weakly Supervised Framework Experiments Framework (WSEF)** [76]: the method generates pseudo-labels by applying different rank correlation measures (e.g., Jaccard, Spearman). The approach is mainly based on the idea that elements that have ranked lists with a high intersection with others probably belong to the same class. The implementation<sup>7</sup> provided by the authors was used considering Rank Biased Overlap (RBO) [77]

correlation measure,  $k = 40$  in combination with SVM.

- **CoMatch** [58]: the method is based on concepts of graph-based self-supervised learning. The approach is trained to produce similar embeddings for the same image with different augmentations. CoMatch jointly optimizes three losses: (i) a supervised classification loss on labeled data, (ii) an unsupervised classification loss on unlabeled data, and (iii) a graph-based contrastive loss on unlabeled data. It takes images as input instead of features. This version employs ResNet [9] as the backbone. We considered the implementation provided by the authors<sup>8</sup>, with default parameters (the ones used for ImageNet [69] in their code). We trained with a batch size of 25 and 400 epochs

<sup>6</sup><https://github.com/lucfra/LDS-GNN>

<sup>7</sup><https://github.com/UDLF/WSEF>

<sup>8</sup><https://github.com/salesforce/CoMatch>

TABLE III: Impact of manifold learning approaches (LHRR, RDPAC, BFSTREE) and Reciprocal Graph (Rec.) on the classification accuracy (%) of 5 different GCN models on CUB200 dataset. The best results for each feature and GCN model are highlighted in bold, the best results for each GCN model are marked with a gray background, and the best result for the entire dataset is highlighted in blue. In all the cases, the best results used manifold learning.

Classifier Specification			Feature			
GCN	Graph	Re-Rank	CNN-ResNet [9]	CNN-SENet [10]	CNN-Xception [74]	VIT-B16 [70]
GCN-Net	kNN	—	40.76 ± 0.7467	35.8 ± 0.0634	46.66 ± 0.019	64.39 ± 0.4486
	kNN	LHRR	49.16 ± 0.3119	36.17 ± 0.1153	51.13 ± 0.0738	70.42 ± 0.671
	kNN	RDPAC	49.44 ± 0.1092	36.84 ± 0.0578	51.18 ± 0.0284	72.71 ± 0.1506
	kNN	BFSTREE	49.18 ± 0.1011	37.10 ± 0.0482	50.62 ± 0.0639	71.54 ± 0.1888
	Rec.	—	49.46 ± 0.3279	<b>39.42 ± 0.113</b>	50.76 ± 0.0713	68.85 ± 0.3055
	Rec.	LHRR	51.23 ± 0.0788	36.5 ± 0.0728	51.92 ± 0.0546	73.49 ± 0.1879
	Rec.	RDPAC	<b>51.57 ± 0.0999</b>	38.57 ± 0.0712	<b>53.12 ± 0.0596</b>	<b>74.39 ± 0.3061</b>
	Rec.	BFSTREE	50.80 ± 0.0291	37.8 ± 0.0538	51.82 ± 0.0658	73.58 ± 0.3939
GCN-SGC	kNN	—	47.55 ± 0.0329	36.48 ± 0.0684	48.60 ± 0.0072	74.23 ± 0.0385
	kNN	LHRR	51.22 ± 0.0184	35.88 ± 0.0137	52.36 ± 0.0125	77.84 ± 0.0519
	kNN	RDPAC	51.88 ± 0.0315	37.75 ± 0.0148	52.98 ± 0.0103	78.16 ± 0.0453
	kNN	BFSTREE	51.66 ± 0.016	37.70 ± 0.01	52.21 ± 0.0095	77.31 ± 0.0563
	Rec.	—	53.71 ± 0.0362	<b>40.31 ± 0.0255</b>	54.0 ± 0.0054	78.03 ± 0.0428
	Rec.	LHRR	51.99 ± 0.0251	36.74 ± 0.0162	53.12 ± 0.0153	78.54 ± 0.0177
	Rec.	RDPAC	<b>52.85 ± 0.0164</b>	38.91 ± 0.0073	<b>54.59 ± 0.0036</b>	<b>79.27 ± 0.0325</b>
	Rec.	BFSTREE	52.68 ± 0.0308	38.65 ± 0.023	53.54 ± 0.0041	78.12 ± 0.0344
GCN-GAT	kNN	—	41.84 ± 0.2901	32.5 ± 0.205	42.45 ± 0.1848	59.53 ± 0.5668
	kNN	LHRR	48.86 ± 0.1593	34.78 ± 0.1155	48.8 ± 0.246	64.02 ± 0.4082
	kNN	RDPAC	49.05 ± 0.1145	35.9 ± 0.1158	49.03 ± 0.1037	68.78 ± 0.2495
	kNN	BFSTREE	48.77 ± 0.1427	35.98 ± 0.1457	48.3 ± 0.1084	68.1 ± 0.2488
	Rec.	—	45.46 ± 0.1879	33.02 ± 0.1206	45.88 ± 0.16	64.82 ± 0.2582
	Rec.	LHRR	50.19 ± 0.0904	35.28 ± 0.1364	50.17 ± 0.1073	70.31 ± 0.0762
	Rec.	RDPAC	<b>50.95 ± 0.0632</b>	<b>37.55 ± 0.1087</b>	<b>51.29 ± 0.1577</b>	<b>72.94 ± 0.1716</b>
	Rec.	BFSTREE	49.89 ± 0.1871	36.67 ± 0.129	49.87 ± 0.1245	71.73 ± 0.1775
GCN-APPNP	kNN	—	29.16 ± 0.6867	30.27 ± 0.3694	42.68 ± 0.0826	55.24 ± 0.5689
	kNN	LHRR	47.0 ± 0.1836	34.91 ± 0.1598	48.77 ± 0.0979	66.57 ± 0.572
	kNN	RDPAC	47.19 ± 0.0701	35.29 ± 0.1195	47.72 ± 0.094	69.92 ± 0.2262
	kNN	BFSTREE	46.59 ± 0.2154	35.28 ± 0.0718	47.14 ± 0.0895	70.86 ± 0.2702
	Rec.	—	48.51 ± 0.1192	38.02 ± 0.0461	47.51 ± 0.0452	68.29 ± 0.0935
	Rec.	LHRR	<b>51.99 ± 0.0800</b>	37.45 ± 0.0768	51.43 ± 0.084	74.61 ± 0.0991
	Rec.	RDPAC	51.82 ± 0.1028	<b>39.15 ± 0.1601</b>	<b>52.17 ± 0.0865</b>	<b>75.59 ± 0.2139</b>
	Rec.	BFSTREE	50.6 ± 0.0848	38.21 ± 0.0358	50.26 ± 0.1301	74.15 ± 0.1837
GCN-ARMA	kNN	—	38.74 ± 0.4527	32.96 ± 0.1626	42.91 ± 0.1465	60.26 ± 0.4398
	kNN	LHRR	47.58 ± 0.2387	34.56 ± 0.0799	49.26 ± 0.2191	67.21 ± 0.2825
	kNN	RDPAC	47.77 ± 0.2075	35.4 ± 0.1474	49.88 ± 0.1479	71.16 ± 0.2337
	kNN	BFSTREE	47.12 ± 0.3126	35.6 ± 0.1385	48.78 ± 0.0991	70.13 ± 0.4433
	Rec.	—	44.37 ± 0.1739	34.25 ± 0.1559	46.95 ± 0.3062	64.55 ± 0.3184
	Rec.	LHRR	49.29 ± 0.0987	35.22 ± 0.0891	50.38 ± 0.1318	70.05 ± 0.653
	Rec.	RDPAC	<b>49.81 ± 0.2090</b>	<b>37.12 ± 0.1276</b>	<b>51.63 ± 0.1155</b>	<b>73.29 ± 0.34</b>
	Rec.	BFSTREE	48.92 ± 0.2721	36.38 ± 0.1331	50.41 ± 0.0777	72.17 ± 0.3336

for all datasets. Except for the CUB200 dataset, which is larger, we used a batch size of 50 and 300 epochs.

We also compared our results with three CNN-based classifiers, considering image data as input. The images were provided with a size of 100x100 pixels in batches of size 32. For the other methods, the input consists of feature vectors obtained from deep features trained through transfer learning. Notice that the CNNs used as baselines require more labeled data in comparison to other methods and were evaluated on a supervised cross-validation scenario (9 folds for training, 1 fold for testing). Except for CNN classifiers, all other methods were evaluated on semi-supervised scenarios (1 fold

for training, 9 folds for testing).

Table IV presents the comparison with both traditional and recent state-of-the-art baselines in relation to our approach on Flowers, Corel5k, and CUB200 datasets. Most results are the mean of 5 executions of 10 folds, with some exceptions which are indicated in italic text. Some methods require long running times on larger datasets (i.e., LDS and CoMatch). For GNN-KNN-LDS, KNN-LDS, and CoMatch, the results on CUB200 correspond to 1 execution. For CoMatch, the mean of 3 executions is reported for Corel5k dataset. The best result for each feature is highlighted in bold and the best for each dataset is highlighted in red. The gray rows indicate the results

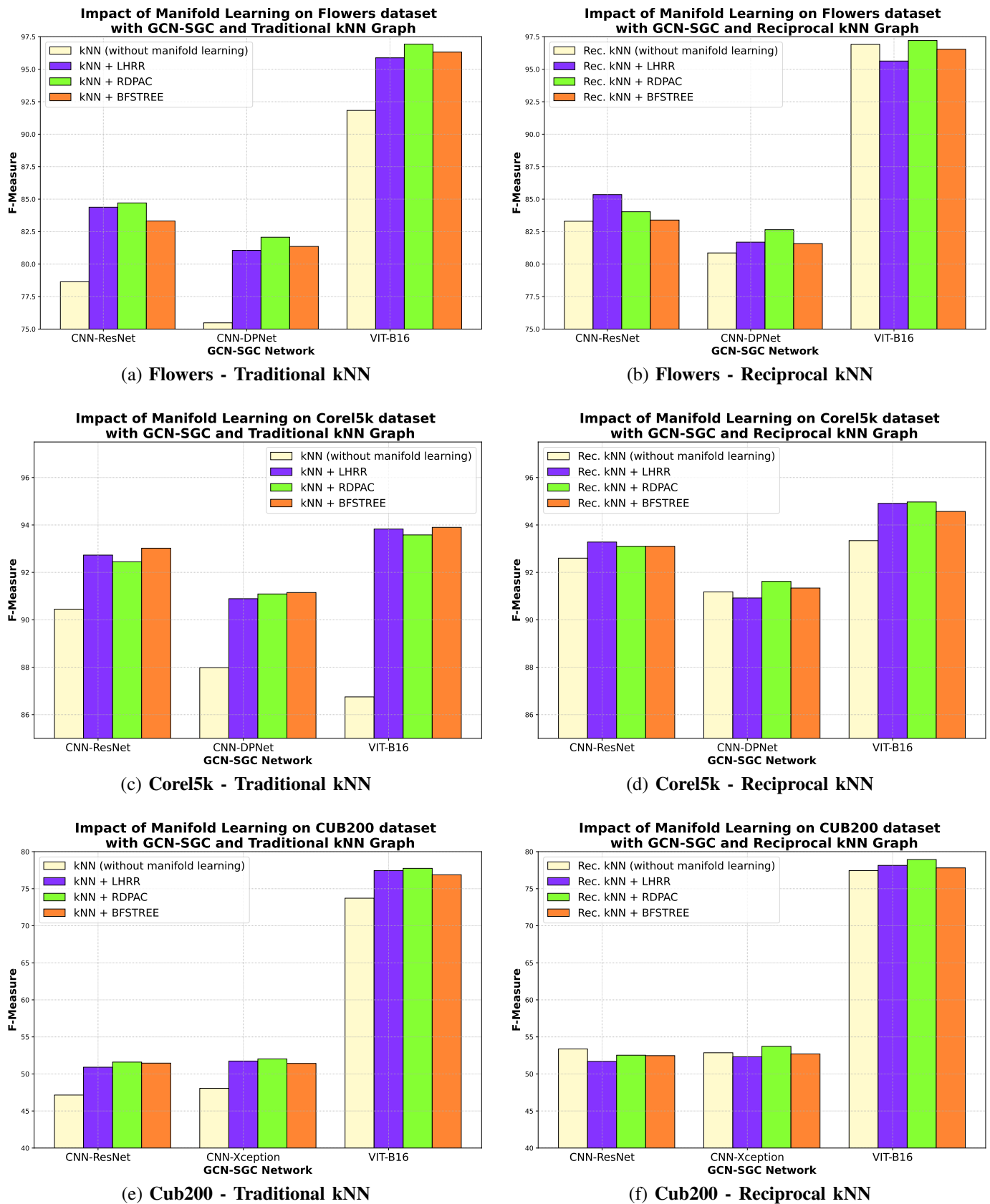


Fig. 2: Impact of manifold learning approaches on F-measure results considering GCN-SGC on different datasets and features.

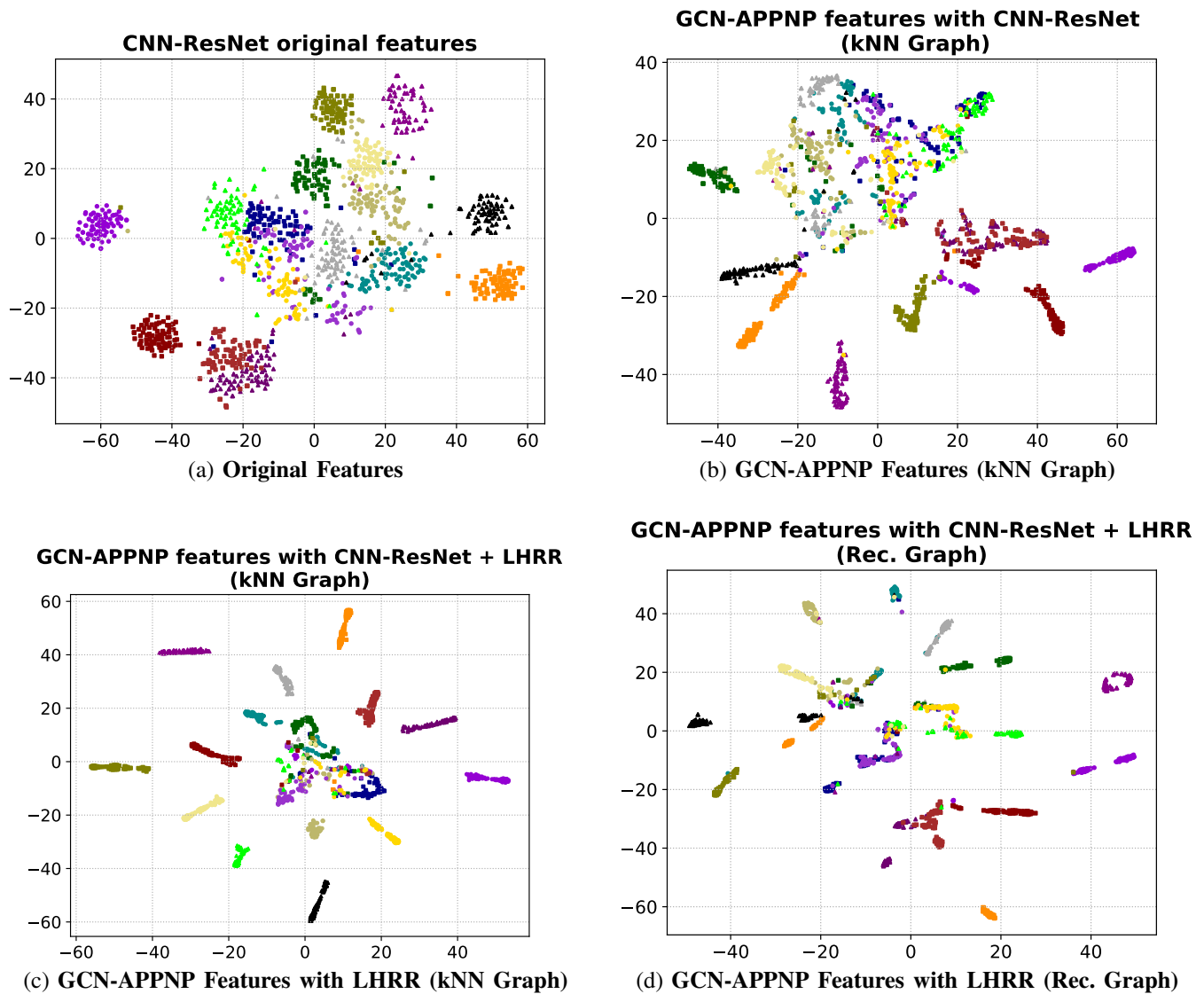


Fig. 3: t-SNE visualizations that show the feature space improvement when manifold learning and reciprocal graph were applied. Experiments were conducted on the Flowers dataset and CNN-ResNet features. Each class is represented by a different shape and color.

that correspond to our method.

The proposed method revealed superior results compared to the baselines in most of the cases. The only exception is Flowers with ViT-B16 features where WSEF shows the best results (97.82% accuracy). However, our ManifoldGCN is very close with 97.43% accuracy.

#### F. Efficiency Results

We conducted an experiment to measure the run-time (in seconds) for running each of the manifold learning methods and GCN models. The experiments were executed on a machine with an Intel(R) Core(TM) i7-10700F CPU @ 2.90GHz, 32 GB RAM, NVIDIA GeForce RTX 3060 GPU with 12GB VRAM running Ubuntu 20.04 with Linux kernel 5.15.0-52-generic. Table V reports the average and standard deviation of

5 executions of 10 folds on each dataset and for the two types of graphs ( $kNN$  and Reciprocal  $kNN$ ).

Manifold Learning (M.L.) performs the pre-processing of the GCN graph. Since these methods are not currently parallelized, they run all on CPU. Parallelization of these approaches is out of the scope of this paper, but rank-based methods can be parallelized with data parallelism as shown in other papers [18], [78]. While the training involves both the GCN initialization and the learning process, testing is responsible for computing the classification of all the queries. Both training and testing are performed on the GPU.

Notice that the execution times are very low, which indicates that the method is fast even for the more robust GCNs. Also, most compared methods have a costly training process. An example is CoMatch (2021) that requires huge training times: 40 minutes on Flowers; 88.4 minutes on Core15k; 260 minutes

TABLE IV: Accuracy comparison (%) for baselines on Flowers, Corel5k, and CUB200 datasets. For every dataset, we compared our approach with both supervised and semi-supervised baselines. The methods are compared with different input features. The results of our method are highlighted with a gray background; the best results for each pair of features and dataset are marked in bold, and the best results for each dataset are in red.

Method	Year	Input	Training	Flowers	Corel5k	CUB200
MobileNet	2017	Images	Supervised	86.66	90.90	35.20
ResNet50	2015			85.97	91.52	31.10
CNN-Xception	2016			90.24	93.32	44.25
CoMatch	2021	Images	Semi-Supervised	82.55	85.70	38.29
kNN	—	ResNet Features	Semi-Supervised	63.67	76.80	36.67
SVM	1995			80.54	88.73	48.84
OPF	2009			71.77	83.56	38.59
SL-Perceptron	—			75.44	83.56	39.91
ML-Perceptron	—			78.88	87.10	32.24
PseudoLabel+SGD	2013			82.69	89.76	21.67
LS+kNN	2004			73.49	83.98	36.99
LS+SVM	2004			73.53	83.26	38.70
LS+OPF	2004			72.66	82.32	39.28
LS+SL-Perceptron	2004			72.34	82.38	39.21
LS+ML-Perceptron	2004			73.03	82.53	39.68
GNN-LDS	2019			54.98	62.69	—
GNN-KNN-LDS	2019			79.32	88.94	37.78
WSEF+SVM+RBO	2021			85.12	91.68	52.17
SGC+Rec.+RDPAC	Ours			84.53	92.00	<b>52.85</b>
ManifoldGCN (best result)	Ours	<b>85.88</b>	<b>93.08</b>	<b>52.85</b>		
kNN	—	SENet Features	Semi-Supervised	48.71	58.78	22.23
SVM	1995			73.30	85.89	35.32
OPF	2009			64.00	81.33	30.94
SL-Perceptron	—			71.84	82.28	36.39
ML-Perceptron	—			72.62	86.90	32.15
PseudoLabel+SGD	2013			76.87	89.85	20.96
LS+kNN	2004			58.05	72.16	20.00
LS+SVM	2004			59.84	72.79	24.82
LS+OPF	2004			59.25	72.20	25.38
LS+SL-Perceptron	2004			59.27	72.19	25.41
LS+ML-Perceptron	2004			59.39	72.24	25.72
GNN-LDS	2019			52.24	65.80	—
GNN-KNN-LDS	2019			73.69	89.95	—
WSEF+SVM+RBO	2021			76.16	89.74	36.49
SGC+Rec.+RDPAC	Ours			76.93	90.85	38.91
ManifoldGCN (best result)	Ours	<b>78.82</b>	<b>92.79</b>	<b>40.31</b>		
kNN	—	ViT-B16 Features	Semi-Supervised	91.91	81.19	56.62
SVM	1995			96.75	91.92	75.61
OPF	2009			96.50	90.02	73.27
SL-Perceptron	—			75.79	82.15	70.84
ML-Perceptron	—			92.59	74.41	12.02
PseudoLabel+SGD	2013			96.84	89.07	30.19
LS+kNN	2004			95.74	89.63	66.15
LS+SVM	2004			94.49	87.59	66.81
LS+OPF	2004			94.22	86.14	66.68
LS+SL-Perceptron	2004			93.71	86.31	65.45
LS+ML-Perceptron	2004			95.13	87.68	62.81
GNN-LDS	2019			72.03	56.33	22.75
GNN-KNN-LDS	2019			96.66	88.56	52.42
WSEF+SVM+RBO	2021			<b>97.82</b>	94.00	78.64
SGC+Rec.+RDPAC	Ours			97.11	95.50	<b>79.27</b>
ManifoldGCN (best result)	Ours	97.43	<b>95.57</b>	<b>79.27</b>		

on CUB200. These times are the average of executions for 100 epochs. However, CoMatch is generally recommended to be trained for 400 epochs. These values are much higher than our proposed approach.

TABLE V: Execution time (in seconds) for manifold learning methods and GCN approaches for both training and testing.

		Flowers	Corel5k	CUB200
ML.	LHRR	1.10 ± 0.0012	6.21 ± 0.0017	20.16 ± 0.0108
	RDPAC	4.66 ± 0.0195	41.74 ± 0.0158	104.18 ± 0.5091
	BFSTREE	9.34 ± 0.0046	37.94 ± 0.1712	95.09 ± 0.0704
Train	GCN-Net (kNN)	0.76 ± 0.0187	2.23 ± 0.0178	6.95 ± 0.0141
	GCN-Net (Rec.)	0.61 ± 0.0016	1.57 ± 0.0018	4.40 ± 0.0003
	GCN-SGC (kNN)	0.15 ± 0.0005	0.20 ± 0.0011	0.54 ± 0.0006
	GCN-SGC (Rec.)	0.14 ± 0.0003	0.19 ± 0.0022	0.51 ± 0.0002
	GCN-GAT (kNN)	3.41 ± 0.0021	11.89 ± 0.0031	30.62 ± 0.0095
	GCN-GAT (Rec.)	2.44 ± 0.0025	7.90 ± 0.0029	19.35 ± 0.0043
	GCN-APPNP (kNN)	0.77 ± 0.0088	3.49 ± 0.0032	27.95 ± 0.0025
	GCN-APPNP (Rec.)	0.75 ± 0.0002	2.44 ± 0.0032	17.11 ± 0.0032
	GCN-ARMA (kNN)	3.84 ± 0.0064	14.45 ± 0.0215	47.8 ± 0.0146
	GCN-ARMA (Rec.)	2.80 ± 0.0051	9.94 ± 0.0013	30.51 ± 0.0113
Test	GCN-Net (kNN)	0.06 ± 0.0366	0.18 ± 0.0382	0.40 ± 0.0327
	GCN-Net (Rec.)	0.05 ± 0.0013	0.18 ± 0.002	0.44 ± 0.0029
	GCN-SGC (kNN)	0.04 ± 0.0015	0.16 ± 0.0011	0.38 ± 0.0051
	GCN-SGC (Rec.)	0.05 ± 0.0015	0.18 ± 0.0018	0.44 ± 0.0005
	GCN-GAT (kNN)	0.04 ± 0.001	0.15 ± 0.0009	0.38 ± 0.004
	GCN-GAT (Rec.)	0.05 ± 0.0015	0.18 ± 0.002	0.44 ± 0.0032
	GCN-APPNP (kNN)	0.05 ± 0.0015	0.15 ± 0.0008	0.38 ± 0.0045
	GCN-APPNP (Rec.)	0.05 ± 0.0015	0.18 ± 0.0021	0.44 ± 0.0026
	GCN-ARMA (kNN)	0.04 ± 0.0015	0.15 ± 0.0008	0.39 ± 0.0036
	GCN-ARMA (Rec.)	0.04 ± 0.0018	0.18 ± 0.0023	0.44 ± 0.0004

## VII. CONCLUSIONS

In this work, we presented a novel framework, the Manifold-GCN, for semi-supervised image classification. The approach is flexible and allows the use of different types of GCNs, graphs, features, and manifold learning. To the best of our knowledge, this is the first framework that allows the combination of GCNs with different types of manifold learning approaches for image classification. In our work, all the manifold learning algorithms are completely unsupervised, which is especially useful for scenarios where labeled data is limited.

An experimental evaluation was conducted on 3 datasets and 5 distinct deep learning features, including features obtained by CNNs and Visual Transformers. The results validated our main hypothesis by revealing that the manifold learning methods were capable of improving the effectiveness (accuracy and F-Measure) in the vast majority of the cases, for different GCNs and features. The visual analyzes show that the feature space was significantly improved by the proposed approach. In comparison to both traditional and very recent state-of-the-art methods, it is clearly noticeable that Manifold-GCN is among the best in most cases. Our approach is also very efficient and requires very low execution times for training and testing.

In future work, we intend to use other types of graph models in addition to kNN Graph and Reciprocal Graph. For this work, the input feature and the feature used to model the graph are the same. Since complementary features can possibly increase results even further, we intend to evaluate cases where a different feature can be used for the graph. We also intend to employ Manifold-GCN in larger image collections and retrieval scenarios. For efficiency purposes, it is also possible to parallelize the implementations of manifold learning approaches.

## ACKNOWLEDGMENTS

The authors are grateful to Fulbright Commission, São Paulo Research Foundation - FAPESP (grants #2017/25908-6, #2018/15597-6, and #2020/11366-0), Brazilian National Council for Scientific and Technological Development - CNPq (grant #309439/2020-5), Petrobras (grant #2017/00285-6), and Microsoft Research for financial support. We also acknowledge the NSF Grant No. IIS-2107213.

## REFERENCES

- [1] R. Datta, D. Joshi, J. Li, and J. Z. Wang, "Image retrieval: Ideas, influences, and trends of the new age," *ACM Computing Surveys*, vol. 40, no. 2, pp. 5:1–5:60, 2008.
- [2] S. Karanam, M. Gou, Z. Wu, A. Rates-Borras, O. Camps, and R. J. Radke, "A systematic evaluation and benchmark for person re-identification: Features, metrics, and datasets," *IEEE Transactions on Pattern Analysis and Machine Intelligence*, vol. 41, no. 3, pp. 523–536, March 2019.
- [3] M. Agarwal and J. Mostafa, "Content-based image retrieval for alzheimer's disease detection," in *2011 9th International Workshop on Content-Based Multimedia Indexing (CBMI)*, June 2011, pp. 13–18.
- [4] M. Sultana and M. Gavrilova, *A Content Based Feature Combination Method for Face Recognition*. Heidelberg: Springer International Publishing, 2013, pp. 197–206.
- [5] M. Wang and T. Song, "Remote sensing image retrieval by scene semantic matching," *IEEE Transactions on Geoscience and Remote Sensing*, vol. 51, no. 5, pp. 2874–2886, May 2013.
- [6] J.-P. Schober, T. Hermes, and O. Herzog, "Content-based image retrieval by ontology-based object recognition," in *KI-2004 Workshop on Applications of Description Logics*, 2004, pp. 61–67.
- [7] M. L. Kherfi and D. Ziou, "Relevance feedback for cbir: a new approach based on probabilistic feature weighting with positive and negative examples," *IEEE Transactions on Image Processing*, vol. 15, no. 4, pp. 1017–1030, April 2006.
- [8] L. Piras and G. Giacinto, "Information fusion in content based image retrieval," *Inf. Fusion*, vol. 37, no. C, p. 50–60, sep 2017.
- [9] K. He, X. Zhang, S. Ren, and J. Sun, "Deep residual learning for image recognition," in *2016 IEEE Conference on Computer Vision and Pattern Recognition (CVPR)*, 2016, pp. 770–778.
- [10] Y. Chen, J. Li, H. Xiao, X. Jin, S. Yan, and J. Feng, "Dual path networks," in *Advances in Neural Information Processing Systems 30*, I. Guyon, U. V. Luxburg, S. Bengio, H. Wallach, R. Fergus, S. Vishwanathan, and R. Garnett, Eds. Curran Associates, Inc., 2017, pp. 4467–4475.
- [11] L. Deng, "A tutorial survey of architectures, algorithms, and applications for deep learning," *APSIPA Transactions on Signal and Information Processing*, vol. 3, 2014.
- [12] M. Sandler, A. Howard, M. Zhu, A. Zhmoginov, and L. Chen, "Mobilenetv2: Inverted residuals and linear bottlenecks," in *2018 IEEE/CVF Conference on Computer Vision and Pattern Recognition*, 2018, pp. 4510–4520.
- [13] M. Ye, J. Shen, G. Lin, T. Xiang, L. Shao, and S. C. H. Hoi, "Deep learning for person re-identification: A survey and outlook," 2020.
- [14] A. Krizhevsky, I. Sutskever, and G. E. Hinton, "Imagenet classification with deep convolutional neural networks," in *Proceedings of the 25th International Conference on Neural Information Processing Systems - Volume 1*, ser. NIPS'12, 2012, pp. 1097–1105.
- [15] O. Sener and S. Savarese, "Active learning for convolutional neural networks: A core-set approach," in *International Conference on Learning Representations*, 2018.
- [16] H. Hino, "Active learning: Problem settings and recent developments," *arXiv:2012.04225v2*, 2020.
- [17] Y. Li, Z. Wu, S. Karanam, and R. Radke, "Real-world re-identification in an airport camera network," 11 2014, pp. 1–6.
- [18] L. P. Valem, D. C. G. Pedronette, and J. Almeida, "Unsupervised similarity learning through cartesian product of ranking references," *Pattern Recognition Letters*, 2017.
- [19] D. C. G. Pedronette, L. P. Valem, J. Almeida, and R. da S. Torres, "Multimedia retrieval through unsupervised hypergraph-based manifold ranking," *IEEE Transactions on Image Processing*, vol. 28, no. 12, pp. 5824–5838, 2019.

- [20] D. C. Guimarães Pedronette, L. Pascotti Valem, and L. J. Latecki, “Efficient rank-based diffusion process with assured convergence,” *Journal of Imaging*, vol. 7, no. 3, 2021.
- [21] M. Li, X. Zhu, and S. Gong, “Unsupervised tracklet person re-identification,” *IEEE Transactions on Pattern Analysis and Machine Intelligence*, 2019.
- [22] Z. Wang, S. Wang, S. Yang, H. Li, J. Li, and Z. Li, “Weakly supervised fine-grained image classification via gaussian mixture model oriented discriminative learning,” in *IEEE/CVF Conference on Computer Vision and Pattern Recognition (CVPR)*, June 2020.
- [23] D. Mandal, P. Rao, and S. Biswas, “Semi-supervised cross-modal retrieval with label prediction,” *IEEE Transactions on Multimedia*, vol. 22, no. 9, pp. 2345–2353, 2020.
- [24] T. N. Kipf and M. Welling, “Semi-supervised classification with graph convolutional networks,” in *5th International Conference on Learning Representations, ICLR 2017, Toulon, France, April 24-26, 2017, Conference Track Proceedings*. OpenReview.net, 2017.
- [25] Z.-H. Zhou, “A brief introduction to weakly supervised learning,” *National Science Review*, vol. 5, no. 1, pp. 44–53, 08 2017.
- [26] Z. Wu, S. Pan, F. Chen, G. Long, C. Zhang, and P. S. Yu, “A comprehensive survey on graph neural networks,” *IEEE Transactions on Neural Networks and Learning Systems*, vol. 32, no. 1, pp. 4–24, 2021.
- [27] A. Sharma, E. Vans, D. Shigemizu, K. A. Borovovich, and T. Tsunoda, “Deepinsight: A methodology to transform a non-image data to an image for convolution neural network architecture,” *Scientific Reports*, vol. 9, no. 1, p. 11399, Aug 2019.
- [28] P. Veličković, G. Cucurull, A. Casanova, A. Romero, P. Liò, and Y. Bengio, “Graph attention networks,” in *International Conference on Learning Representations*, 2018.
- [29] F. Wu, A. Souza, T. Zhang, C. Fifty, T. Yu, and K. Weinberger, “Simplifying graph convolutional networks,” in *Proceedings of the 36th International Conference on Machine Learning*, ser. Proceedings of Machine Learning Research, K. Chaudhuri and R. Salakhutdinov, Eds., vol. 97. PMLR, 09–15 Jun 2019, pp. 6861–6871.
- [30] J. Klicpera, A. Bojchevski, and S. Günnemann, “Combining neural networks with personalized pagerank for classification on graphs,” in *International Conference on Learning Representations*, 2019.
- [31] F. M. Bianchi, D. Grattarola, L. Livi, and C. Alippi, “Graph neural networks with convolutional arna filters,” *IEEE Transactions on Pattern Analysis and Machine Intelligence*, pp. 1–1, 2021.
- [32] L. Nie, Y. Li, F. Feng, X. Song, M. Wang, and Y. Wang, “Large-scale question tagging via joint question-topic embedding learning,” *ACM Trans. Inf. Syst.*, vol. 38, no. 2, feb 2020.
- [33] L. Nie, F. Jiao, W. Wang, Y. Wang, and Q. Tian, “Conversational image search,” *IEEE Transactions on Image Processing*, vol. 30, pp. 7732–7743, 2021.
- [34] L. Franceschi, M. Niepert, M. Pontil, and X. He, “Learning discrete structures for graph neural networks,” in *Proceedings of the 36th International Conference on Machine Learning*, 2019.
- [35] S.-B. Chen, X.-Z. Tian, C. H. Q. Ding, B. Luo, Y. Liu, H. Huang, and Q. Li, “Graph convolutional network based on manifold similarity learning,” *Cognitive Computation*, vol. 12, no. 6, p. 1144, 2020.
- [36] Q. Li, Z. Han, and X. Wu, “Deeper insights into graph convolutional networks for semi-supervised learning,” in *Proceedings of the Thirty-Second AAAI Conference on Artificial Intelligence (AAAI-18)*, S. A. McIlraith and K. Q. Weinberger, Eds., vol. 32, no. 1. AAAI Press, 2018, pp. 3538–3545.
- [37] S. Bai, F. Zhang, and P. H. S. Torr, “Hypergraph convolution and hypergraph attention,” *CoRR*, vol. abs/1901.08150, 2019.
- [38] U. Chaudhuri, B. Banerjee, and A. Bhattacharya, “Siamese graph convolutional network for content based remote sensing image retrieval,” *Computer Vision and Image Understanding*, vol. 184, pp. 22–30, 2019.
- [39] J. Yang, W.-S. Zheng, Q. Yang, Y.-C. Chen, and Q. Tian, “Spatial-temporal graph convolutional network for video-based person re-identification,” in *IEEE Conference on Computer Vision and Pattern Recognition (CVPR)*, 2020, pp. 3286–3296.
- [40] C. Liu, G. Yu, M. Volkovs, C. Chang, H. Rai, J. Ma, and S. K. Gorti, “Guided similarity separation for image retrieval,” in *Advances in Neural Information Processing Systems*, H. Wallach, H. Larochelle, A. Beygelzimer, F. d’Alché-Buc, E. Fox, and R. Garnett, Eds., vol. 32. Curran Associates, Inc., 2019.
- [41] G. Zhang, J. Pan, Z. Zhang, H. Zhang, C. Xing, B. Sun, and M. Li, “Hybrid graph convolutional network for semi-supervised retinal image classification,” *IEEE Access*, vol. 9, pp. 35 778–35 789, 2021.
- [42] J. Jiang, B. Wang, and Z. Tu, “Unsupervised metric learning by self-smoothing operator,” in *2011 International Conference on Computer Vision*, 2011, pp. 794–801.
- [43] J. E. van Engelen and H. H. Hoos, “A survey on semi-supervised learning,” *Machine Learning*, vol. 109, pp. 373–440, 2019.
- [44] A. Vanyan and H. Khachatryan, “Deep semi-supervised image classification algorithms: a survey,” *JUCS - Journal of Universal Computer Science*, vol. 27, no. 12, pp. 1390–1407, 2021.
- [45] D. Zhou, O. Bousquet, T. N. Lal, J. Weston, and B. Schölkopf, “Learning with local and global consistency,” in *Advances in Neural Information Processing Systems 16*. MIT Press, 2004, pp. 321–328.
- [46] D.-H. Lee, “Pseudo-label: The simple and efficient semi-supervised learning method for deep neural networks,” in *Workshop on challenges in representation learning, ICML*, vol. 3, no. 2, 2013.
- [47] C. Cortes and V. Vapnik, “Support-vector networks,” *Mach. Learn.*, vol. 20, no. 3, pp. 273–297, Sep. 1995.
- [48] W. P. Amorim, A. X. Falcão, and M. H. d. Carvalho, “Semi-supervised pattern classification using optimum-path forest,” in *2014 27th SIB-GRAPI Conference on Graphics, Patterns and Images*, Aug 2014, pp. 111–118.
- [49] S. Laine and T. Aila, “Temporal ensembling for semi-supervised learning,” in *International Conference on Learning Representations*, 2017.
- [50] A. Tarvainen and H. Valpola, “Mean teachers are better role models: Weight-averaged consistency targets improve semi-supervised deep learning results,” in *Proceedings of the 31st International Conference on Neural Information Processing Systems*, ser. NIPS’17. Red Hook, NY, USA: Curran Associates Inc., 2017, p. 1195–1204.
- [51] T. Miyato, S. ichi Maeda, M. Koyama, and S. Ishii, “Virtual adversarial training: A regularization method for supervised and semi-supervised learning,” *IEEE Transactions on Pattern Analysis and Machine Intelligence*, vol. 41, pp. 1979–1993, 2019.
- [52] Q. Xie, Z. Dai, E. Hovy, M.-T. Luong, and Q. V. Le, “Unsupervised data augmentation for consistency training,” in *Proceedings of the 34th International Conference on Neural Information Processing Systems*, ser. NIPS’20. Red Hook, NY, USA: Curran Associates Inc., 2020.
- [53] D. Berthelot, N. Carlini, I. J. Goodfellow, N. Papernot, A. Oliver, and C. Raffel, “Mixmatch: A holistic approach to semi-supervised learning,” *CoRR*, vol. abs/1905.02249, 2019.
- [54] K. Sohn, D. Berthelot, C.-L. Li, Z. Zhang, N. Carlini, E. D. Cubuk, A. Kurakin, H. Zhang, and C. Raffel, “Fixmatch: Simplifying semi-supervised learning with consistency and confidence,” in *Proceedings of the 34th International Conference on Neural Information Processing Systems*, ser. NIPS’20. Red Hook, NY, USA: Curran Associates Inc., 2020.
- [55] D. Berthelot, N. Carlini, E. D. Cubuk, A. Kurakin, K. Sohn, H. Zhang, and C. Raffel, “Remixmatch: Semi-supervised learning with distribution matching and augmentation anchoring,” in *International Conference on Learning Representations*, 2020.
- [56] C. Gong, D. Wang, and Q. Liu, “Alphamatch: Improving consistency for semi-supervised learning with alpha-divergence,” in *2021 IEEE/CVF Conference on Computer Vision and Pattern Recognition (CVPR)*, 2021, pp. 13 678–13 687.
- [57] T. Chen, S. Kornblith, M. Norouzi, and G. Hinton, “A simple framework for contrastive learning of visual representations,” in *Proceedings of the 37th International Conference on Machine Learning*, ser. ICML’20. JMLR.org, 2020.
- [58] J. Li, C. Xiong, and S. C. H. Hoi, “Comatch: Semi-supervised learning with contrastive graph regularization,” in *2021 IEEE/CVF International Conference on Computer Vision (ICCV)*, 2021, pp. 9455–9464.
- [59] B. Kim, J. Choo, Y. Kwon, S. Joe, S. Min, and Y. Gwon, “Self-match: Combining contrastive self-supervision and consistency for semi-supervised learning,” *CoRR*, vol. abs/2101.06480, 2021.
- [60] D. C. G. Pedronette and L. J. Latecki, “Rank-based self-training for graph convolutional networks,” *Information Processing & Management*, vol. 58, no. 2, p. 102443, 2021.
- [61] S. M. Omohundro, “Five balltree construction algorithms,” Tech. Rep., 1989.
- [62] A. Gionis, P. Indyk, and R. Motwani, “Similarity search in high dimensions via hashing,” in *Proceedings of the 25th International Conference on Very Large Data Bases*, ser. VLDB ’99, 1999, p. 518–529.
- [63] F. Pedregosa, G. Varoquaux, A. Gramfort, V. Michel, B. Thirion, O. Grisel, M. Blondel, P. Prettenhofer, R. Weiss, V. Dubourg, J. Vanderplas, A. Passos, D. Cournapeau, M. Brucher, M. Perrot, and E. Duchesnay, “Scikit-learn: Machine learning in Python,” *Journal of Machine Learning Research*, vol. 12, pp. 2825–2830, 2011.

- [64] D. C. G. Pedronette, L. P. Valem, and R. da S. Torres, "A bfs-tree of ranking references for unsupervised manifold learning," *Pattern Recognition*, vol. 111, p. 107666, 2021.
- [65] D. Qin, S. Gammeter, L. Bossard, T. Quack, and L. van Gool, "Hello neighbor: Accurate object retrieval with k-reciprocal nearest neighbors," in *CVPR 2011*, 2011, pp. 777–784.
- [66] M.-E. Nilsback and A. Zisserman, "A visual vocabulary for flower classification," in *Proceedings of the IEEE Conference on Computer Vision and Pattern Recognition*, vol. 2, 2006, pp. 1447–1454.
- [67] G.-H. Liu and J.-Y. Yang, "Content-based image retrieval using color difference histogram," *Pattern Recognition*, vol. 46, no. 1, pp. 188 – 198, 2013.
- [68] C. Wah, S. Branson, P. Welinder, P. Perona, and S. Belongie, "The Caltech-UCSD Birds-200-2011 Dataset," California Institute of Technology, Tech. Rep. CNS-TR-2011-001, 2011.
- [69] J. Deng, W. Dong, R. Socher, L.-J. Li, K. Li, and L. Fei-Fei, "ImageNet: A Large-Scale Hierarchical Image Database," in *CVPR09*, 2009.
- [70] A. Dosovitskiy, L. Beyer, A. Kolesnikov, D. Weissenborn, X. Zhai, T. Unterthiner, M. Dehghani, M. Minderer, G. Heigold, S. Gelly, J. Uszkoreit, and N. Houlsby, "An image is worth 16x16 words: Transformers for image recognition at scale," in *International Conference on Learning Representations*, 2021.
- [71] L. Yuan, Y. Chen, T. Wang, W. Yu, Y. Shi, F. E. Tay, J. Feng, and S. Yan, "Tokens-to-token vit: Training vision transformers from scratch on imagenet," *arXiv preprint arXiv:2101.11986*, 2021.
- [72] L. van der Maaten and G. Hinton, "Visualizing data using t-sne," *Journal of Machine Learning Research*, vol. 9, no. 86, pp. 2579–2605, 2008.
- [73] J. Hu, L. Shen, and G. Sun, "Squeeze-and-excitation networks," in *2018 IEEE Conference on Computer Vision and Pattern Recognition (CVPR)*, 2018.
- [74] F. Chollet, "Xception: Deep learning with depthwise separable convolutions," in *2017 IEEE Conference on Computer Vision and Pattern Recognition (CVPR)*, 2017, pp. 1800–1807.
- [75] J. Papa, A. Falcão, and C. Suzuki, "Supervised pattern classification based on optimum-path forest," *Int. J. Imaging Syst. Technol.*, vol. 19, no. 2, pp. 120–131, Jun. 2009.
- [76] J. G. C. Presotto, L. P. Valem, N. G. de Sá, D. C. G. Pedronette, and J. P. Papa, "Weakly supervised learning through rank-based contextual measures," in *2020 25th International Conference on Pattern Recognition (ICPR)*, 2021, pp. 5752–5759.
- [77] W. Webber, A. Moffat, and J. Zobel, "A similarity measure for indefinite rankings," *ACM Trans. Inf. Syst.*, vol. 28, no. 4, nov 2010.
- [78] L. P. Valem, D. C. G. a. Pedronette, R. d. S. Torres, E. Borin, and J. Almeida, "Effective, efficient, and scalable unsupervised distance learning in image retrieval tasks," in *Proceedings of the 5th ACM on International Conference on Multimedia Retrieval*, ser. ICMR '15. New York, NY, USA: ACM, 2015, pp. 51–58.